

Sensor for direct measurement of the boundary shear stress in fluid flow

Xiaoqi Bao¹, Mircea Badescu, Yoseph Bar-Cohen, Shyh-Shiuh Lih, Stewart Sherrit, Zensheu Chang, Beck Chen, Scott Widholm and Patrick Ostlund

Jet Propulsion Laboratory, California Institute of Technology, (MS 67-119), 4800 Oak Grove Drive, Pasadena, CA 91109-8099, Phone 818-393-5700, Fax 818-393-2879, xbao@jpl.nasa.gov web: <http://ndeaa.jpl.nasa.gov>

ABSTRACT

The formation of scour patterns at bridge piers is driven by the forces at the boundary of the water flow. In most experimental scour studies, indirect processes have been applied to estimate the shear and normal stress using measured velocity profiles. The estimations are based on theoretical models and associated assumptions. However, the turbulence flow fields and boundary layer in the pier-scour region are very complex. In addition, available turbulence models cannot account accurately for the bed roughness effect. Direct measurement of the boundary shear and normal stress and their fluctuations are attractive alternatives. However, this approach is a challenging one especially for high spatial resolution and high fidelity measurements. The authors designed and fabricated a prototype miniature shear stress sensor including an EDM machined floating plate and a high-resolution laser optical encoder. Tests were performed both in air as well as operation in water with controlled flow. The sensor sensitivity, stability and signal-to-noise level were measured and evaluated. The detailed test results and a discussion of future work will be presented in this paper.

KEYWORD: Sensor, shear stress, fluid flow.

1. INTRODUCTION

The flow fields and boundary erosion that are associated with scour at bridge piers are very complex. In particular, scour development is complicated by the important effects of large scale turbulence structures (macro-turbulence) that markedly characterize pier flow fields. The role that such turbulence structures play in scour has only been partially appreciated. It is a role that needs to be very well-understood when investigating scour at bridge piers. Turbulence structures, together with local flow convergence / contractions around the fronts and flanks of piers, or between piles of complex pier configurations, are erosive flow mechanisms of primary importance. The interactions of macro-turbulence structures with themselves and converging flows are of key significance in illuminating how pier geometry affects sediment entrainment and thereby scour morphology and maximum scour depth. The measurement of shear stress has applications in many other problems including the performance and transportation vehicles and surface flow characterization [Naughton and Sheplak, 2002].

Most researchers have applied an indirect process to determine shear stress using precise measured velocity profiles. Laser Doppler Anemometry and Particle Image Velocimetry are common techniques used to accurately measure velocity profiles. These methods are based on theoretical assumptions to estimate boundary shear stress. In addition, available turbulence models cannot very well account for the effect of bed roughness which is fundamentally important for any CFD simulation. Yucel and Graf [1975] developed a method to determine the shear force in a sand-water mixture flow by measuring the voltage required to maintain a flush-mounting hot-film at constant temperature. Qu et al [2008] determined the shear force by measuring the resistance of a carbon nanotube. Tunga et al [2007] used a similar method and a sensor based on laterally aligned carbon nanotubes. Große et al [2006] used elastomeric cylindrical pillars with a diameter of a few microns and a high speed CCD camera to measure pillar's tip deflection.

Direct measurement boundary shear stress and boundary pressure fluctuations in experimental scour research has always been a challenge and almost impossible. This method measures the displacement of a plate due to shear force developed in contact with a flow. Akasofu and Neuman [Akasofu, 1991] used the change of the capacitance of a capacitor bridge to measure the deformation of a silicon gel layer due to shear force. This is relatively simple solution, small scale and easy to seal but the sensitivity, electric shielding and material stability raise issues regarding its use.

¹ Correspondence: xbao@jpl.nasa.gov

Roche et al [1996] developed a sensor based on piezoelectric biomorphs with a plate at the top. It is more applicable to AC shear stress rather than a DC shear stress and so it is difficult to work with at very low frequency.

A shear sensor device that was developed by the TFHRC Hydraulics Research team to measure wall shear stress directly has a large floating plate of 75 mm in diameter. It uses a Hall Effect to detect the displacement of the floating plate. An electric current is applied to a magnetic coil to create a counter force and maintain the displacement to be zero. The required current is used as the measure of the shear stress on the plating plate. The sensor is bulk in size and has low resonance frequency. Therefore, it is limited to measure shear stresses averaged in large area and long time period. The large sensor plate has to be aligned with the channel bed surface and cannot be used to measure shear stress in curved scour holes. There is a need to develop a sensor with higher spacial and time resolution for a sensing system that can measure instantaneous areal boundary shear stresses for scaled bridge scour experiments.

Our approach is to reduce the size and mass of the floating plate for high spatial resolution and broad frequency range and apply high sensitive position sensor to measure the small displacement of the plate induced by the shear force. A fold beam support to the floating place was conceived to reduce the foot print. An optical encoder with resolution of 1.2 nm is selected as the position sensor. Sensors of two implementations were designed and fabricated. The sensors were tested in a water testbed at JPL. Four sensors of second implementation were put in a 2x2 array and tested in a water flume at Turner Fairbanks Highway Research Center (TFHRC) of Federal Highway Administration (FHWA), DoT.

2. Sensor design, fabrication, and instrumentation

The first implementation has a floating plate with effected floating part of 7.1x7.8 mm and uses encoder MicroE MII5800. The structure of the floating plate is shown in Figure 1. The primary experimental investigation of the performance of this implement in air was reported in a previous paper [Badescu et al 2010]. The floating plate of the second implementation has the same structure as the first implementation. To increase the signal level the second implement increases the effective floating area to 11.7x10.9 mm and uses new model of encoder MII6800, which removed partial electronics from the sensor head and reduced the heat generation. The sensors were designed to construct an array. The details of the structure are shown in Figure 2 and the 2x2 array is shown in Figure 3. A pressure sensor located at the center of the array was added for monitoring the dynamic pressure of the turbulence flow.

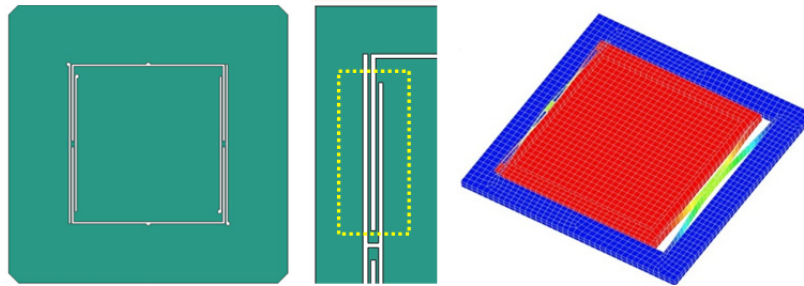


Figure 1: Sensor plate design with flexure blades detail and FEA model.

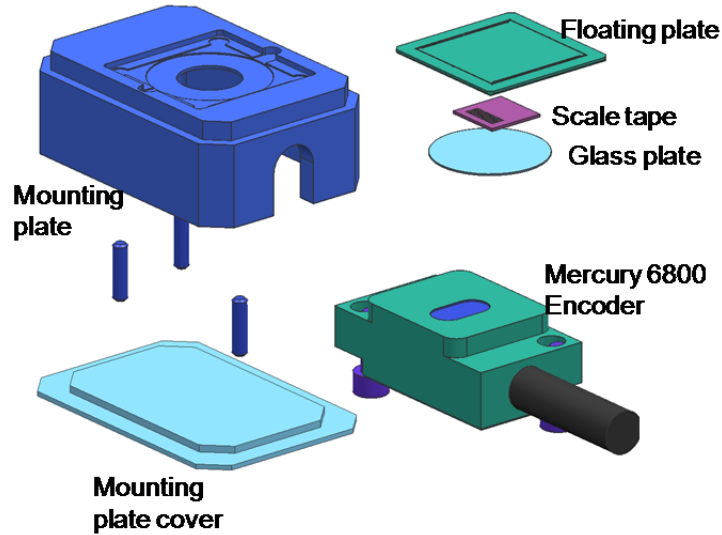


Figure 2: Encapsulated array element shear sensor design

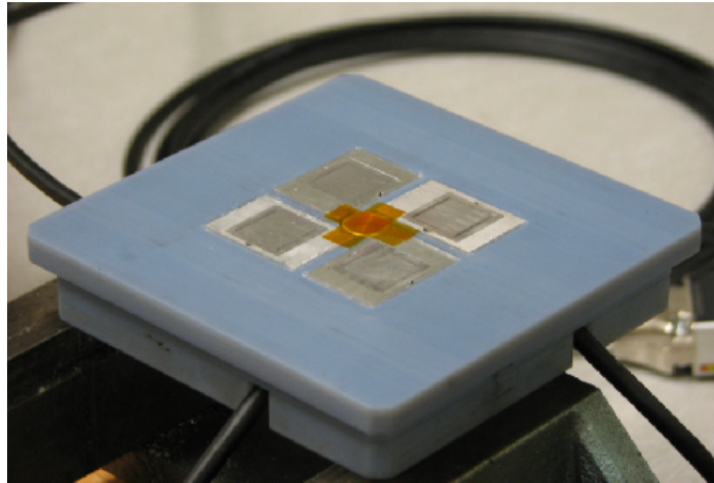


Figure 3: 2x2 Array mounted on a plastic plate

3. Sensitivity calibration of the sensors

The force sensitivities of the sensors were calibrated utilizing gravity force of the floating part. The shear stress sensitivities were calculated from the force sensitivities by taking the count of the surface area. The sensor was mounted on a rotation table as showed in Figure 4. . The scale on the adjusting wheel is 2" (0.033°) per division. The plate surface of the sensor was leveled to be horizontal by using bobble leveler. The resolution of the bobble leveler is better than 0.2°.

The reading was set to zero when the sensor was horizontally leveled and the readings at 90 and -90 degrees were recorded while the plus or minus of gravity force of the floating part was applied. The mass of the floating part and surface area of the second implement sensors are listed in Table 1 and the sensor output and the calculated sensitivity results for ware listed in the Table 2. The resonance frequencies are calculated from the mass and the measured compliance (nm/N). The compliance of the first implement sensor was calibrated as 1.08e6 nm/N, stress sensitivity 59.8 nm/Pa, and the resonance frequency was calculated as 505 Hz. The stress sensitivities of the second implement sensors are about 6 times of the first implement.

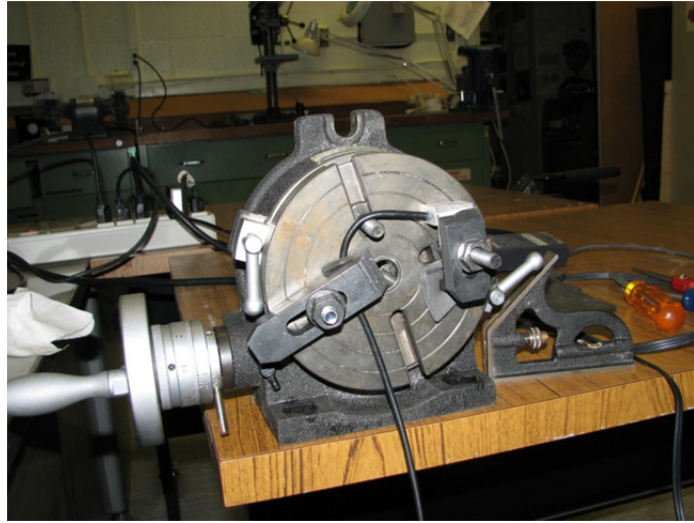


Figure 4: Sensor mounted on rotation table for calibration

Table 1: The Mass and surface area of the floating part of the second implement sensors ceramic

	Total	Floating plate	Scale	Glue	Area	
mg	184	127	47	10	127.1	mm ²

Table 2: Summary of the calibration results of the four second implement sensors

Sensor	nm +	nm -	nm+/nm-	nm+' - 'nm-'	nm/N	nm/Pa	Count/Pa	Pa/Count	Reson. Hz
#1	6290	-5900	-1.07	12190	3.38E+06	429.0	351.5	0.002845	202
#2	5330	-5170	-1.03	10500	2.91E+06	369.6	302.7	0.003303	218
#3	4690	-4772	-0.98	9462	2.62E+06	333.0	272.8	0.003665	229
#4	5270	-5090	-1.04	10360	2.87E+06	364.6	298.7	0.003348	219
Average					2.94E+06	374.1	306.4	0.003290	217

4. The stability of the sensors

As reported in the previous paper, the thermal shift of output of the sensor was observed after turn on the sensor. The shift amount, curve and the time to reach new thermal equilibrium depend on the heat generated by the sensor head, the heat conducting path and convection condition of the surrounding water and air. For the sensor of first implement, a shift of 140 nm was observed when the sensor was mounted on a stainless optical table in air in following 1 hour after 5 minutes after turning on. However, the shift could be more than 1000 nm when the sensor was on a wood table. In the second implement, new model encoder MII6800 with less power consumption in probe head was used to reduce the thermal shift. Figure 5 shows a test result of the thermal shift after turning on three MII6800 encoders. The encoders were put on a wood table and scale was placed onto the encoder with spacer in between and with a weight on top.

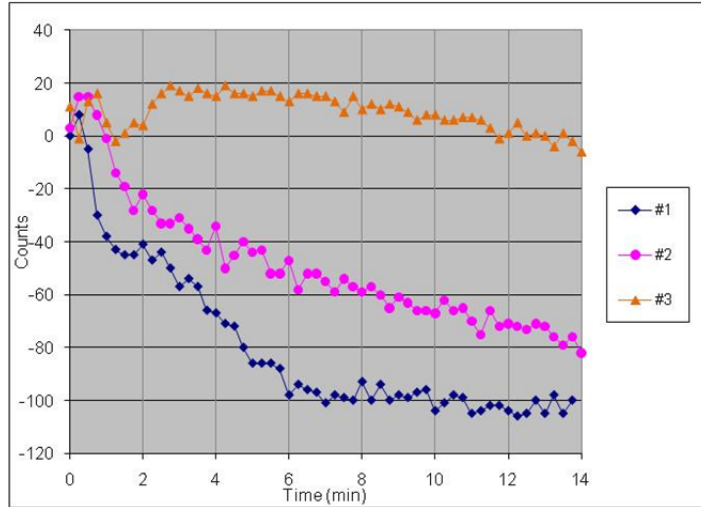


Figure 5: The stability test for three second implement encoders after turning on in air. One count is equaled to 1.2 nm.

In the shear stress measurement the sensor will be in the forced convection condition. The thermal shift caused by water moving was observed. Figure 6 shows an example of the shift of the #1 sensor of the second implement. The water was moved slowly perpendicular to the sensing direction of the sensor by hand with a piece of plastic plate. A shift 140 nm was observed in 20 seconds. The output was shifted to -100 nm in ~60 seconds after stopping the movement and a gradual recovering followed. Comparing with ~2100 nm displacement for a shear stress of 6 Pa, the shift may result in a significant error. Observations also show the averaged output did not change obviously with water moving speed change. Since the heat capacity of the water is relatively large comparing with the heat generated by the encoder head the water moving at slow speed is enough to remove the heat. A reasonable approach to reduce the error of shear stress measurement in water flow is to take the reading just after the flow stopped as the zero reference to correct the data. Another possible approach is to keep a slow water flow in the measurement to maintain convection thermal condition for the sensor. The shear stress is approximately proportional to the square of the speed. A slow speed will not induce significant error to the measurement.

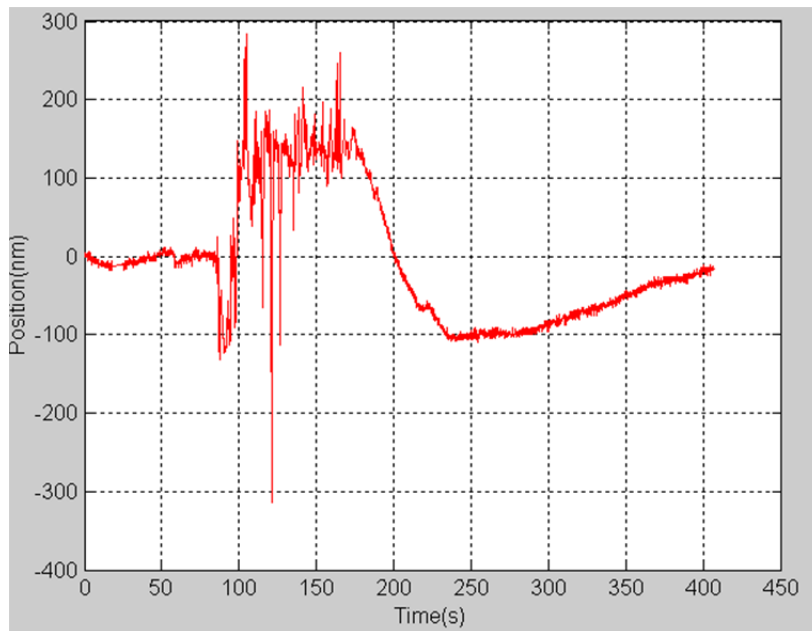


Figure 6: Thermal shift induced by slow water movement perpendicular to sensing direction

5. Test in turbulence water flow

The sensor array was tested in the flume at Turner Fairbanks Highway Research Center (TFHRC) of Federal Highway Administration (FHWA), DOT as shown in Figure 7. Sensing directions of sensors #1 and #3 were along the water flow and sensors #2 and #4 were perpendicular. Water leakage was found through the array and sensor #1 was out of order in the second test day. The sensor #4 showed abnormal big shifts.

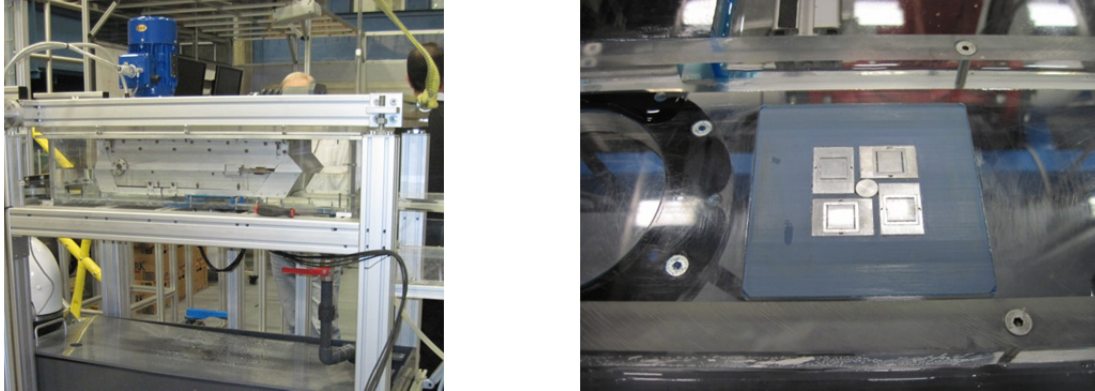


Figure 7: Left: the flume at FHWA of DoT; Right: a close look of the sensor array mounted on the bottom floor

The belt speed was controlled as 2 m/s and the pump motor was driven at 13 Hz. The static water surface was 12” above the sensor surface. Data were recorded in four sequential runs. The low pass filter of the encoder was set as 20 Hz and the sampling rate was 50 Sample/s. Figures 8 shows the shear stress measured by sensor #3 in the four runs respectively and a summary of the results is listed in Table 3. The averaged shear stresses obtained from Runs 2-4 were relatively consistent within $\pm 5\%$. The stress and the standard deviation (STD) recorded in Run 1 is 34% and 23% higher. The causes are not clear at this time. In Run 4 the pump was run slowly before and after the full speed running. It was a trial to maintain the thermal convection condition as mentioned in the previous paragraph. The curve obtained from Run 4 looks better than the other Runs.

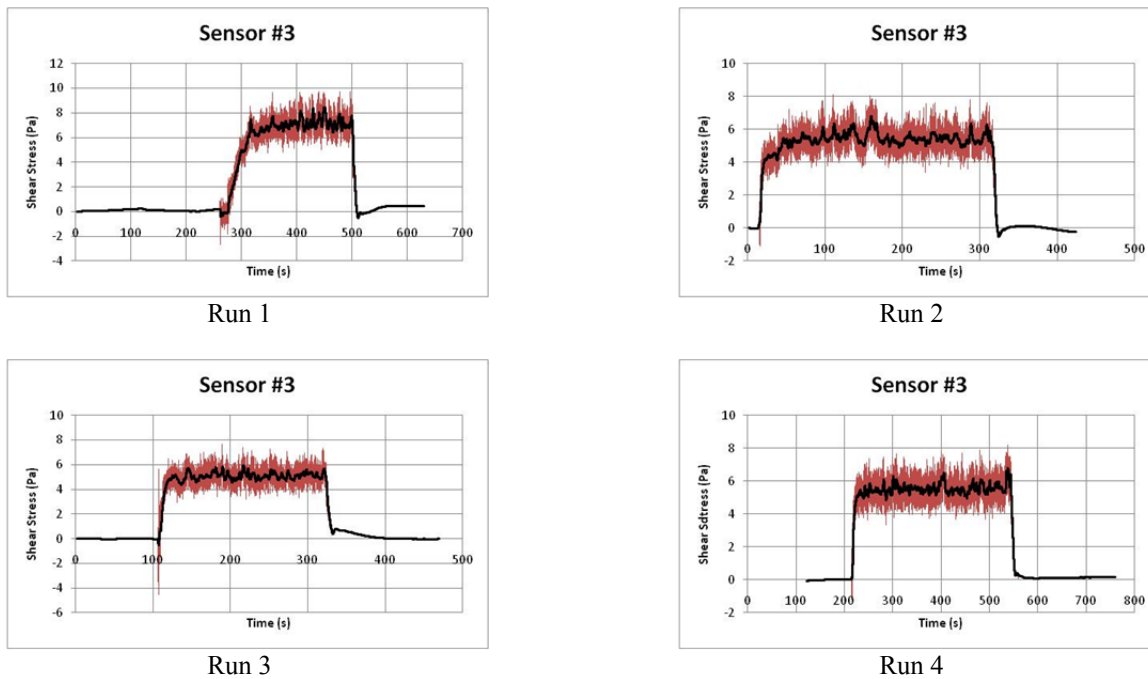


Figure 8: Recorded data of sensor #3 from four sequential runs. The black lines are 100 point moving average.

Table: 3 Summary and comparison of the data of sensor #3 in the four runs:

Run	Average (Pa)	/(2-4 Ave.)	STD (Pa)	/(2-4 Ave.)
1	7.17	1.34	0.74	1.23
2	5.43	1.02	0.62	1.03
3	5.09	0.95	0.61	1.01
4	5.53	1.03	0.58	0.96
2-4 Average	5.35		0.60	

Figures 9 is the corresponding power spectrums density (PSD). The frequency resolution is ~0.1 Hz (50/512 Hz). These curves are similar in general.

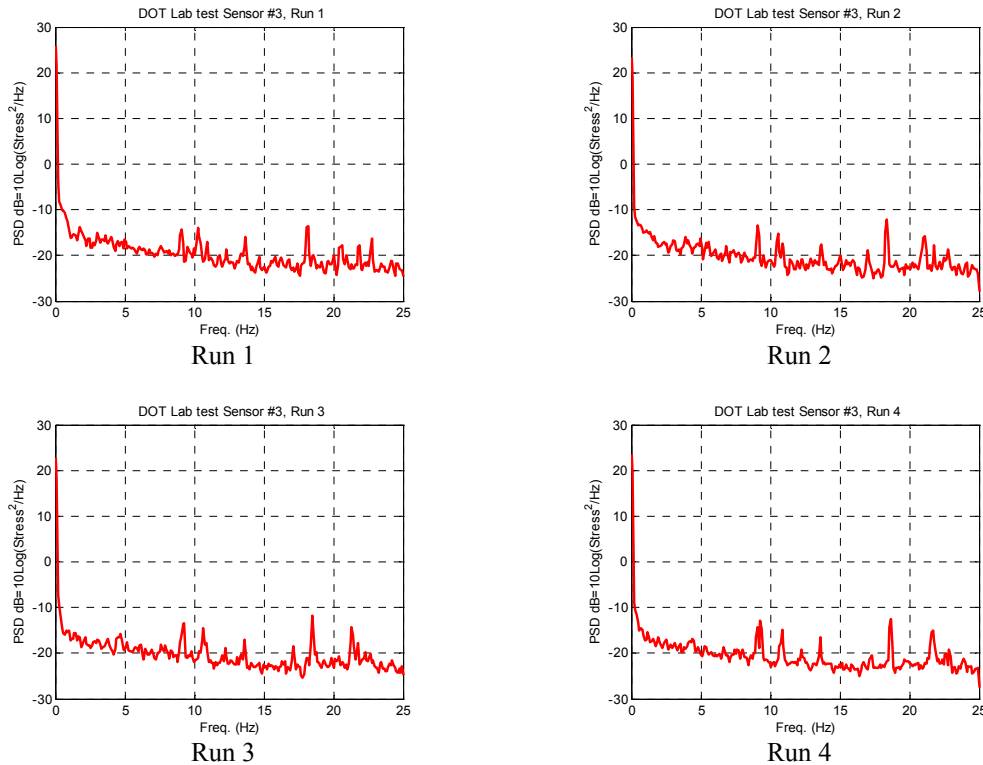


Figure 9: The power spectrums density (PSD) of sensor #3 from four sequential runs.

5. SUMMARY

A novel sensor was developed for direct measurement of shear stress in turbulence water flow. The sensor uses high resolution optical encoder to measure the displacement of small floating plate through a glass window. Relatively high spacial resolution and broad bandwidth were achieved. The possibility to form a compact sensor array was demonstrated. Making the sensor more robust and improve the ratio of signal to other interferences from thermal environment change, pressure change is the future work.

ACKNOWLEDGMENT

The research reported herein was conducted at the Jet Propulsion Laboratory (JPL), California Institute of Technology, under a contract with the National Aeronautics and Space Administration (NASA). This JPL Task Plan No. 82-13107 was conducted under a contract with the Federal Highway Administration, Dept. of Transportation (DoT) entitled "Flexible skin areal shear stress and pressure sensing system for experimental bridge scour research." The authors would like to express their appreciation to Kornel Kerényi, DoT, for his helpful comments, suggestions, and guidance.

REFERENCES

- Akasofu K.-I., and M. R. Neuman, "A Thin-Film Variable Capacitance Shear Force Sensor for Medical and Robotics Applications," *Biosensors*. 9.4-3, 1991, pp. 1601-1602.
- Badescu M., et al, "Direct measurement sensor of the boundary shear stress in fluid flow," *Proceedings of the SPIE Smart Structures Conference*, SPIE Paper 5050-11, San Diego, CA., March (2010)
- Große S., W. Schroder and C. Brucker, "Nano-newton drag sensor based on flexible micro-pillars," *Measurement Science and Technology*, Institute of Physics Publishing Measurement Science and Technology, 17 (2006) 2689–2697 doi:10.1088/0957-0233/17/10/023
- Li, Y., Chandrasekharan, V., Bertolucci, B., Nishida, T., Cattafesta, L., and Sheplak, M., "A MEMS Shear Stress Sensor for Turbulence Measurements," *Proceedings of the 46th AIAA Aerospace Sciences Meeting and Exhibit*, AIAA 2008-269, Reno, Nevada, (7 - 10 January 2008)
- Naughton J.W. and M. Sheplak, "Modern developments in shear stress measurement", *Progress in Aerospace Sciences*, 38, pp. 515-570, 2002
- Qu Y., W. W. Y. Chow, Mengxing Ouyang, Steve C. H. Tung, Wen J. Li, and Xuliang Han, "Ultra-Low-Powered Aqueous Shear Stress Sensors Based on Integrated in Microfluidic Systems," *IEEE Transactions on Nanotechnology*, Vol. 7, No. 5, Sept. 2008 565
- Roche D., C. Richard, L. Eyraud, P. Gonnard, and C. Audoly, "A Piezoelectric Sensor Performing Shear Stress Measurement in an Hydrodynamic Flow," *ISAF 96 (International symposium on the Application of Ferroelectrics)*, UFFC IEEE conference (1996) pp. , 273-276
- Tunga S., H. Rokadiaa, and W. J. Lib "A micro shear stress sensor based on laterally aligned carbon nanotubes," doi:10.1016/j.sna.2006.04.039, *Sensors and Actuators A: Physical*, Volume 133, Issue 2, 12 February 2007, Pages 431-438
- Yucel O., and W. H. Graf, "Wall Shear Measurement in Sand-Water Mixture Flows," *Journal of the Hydraulics Division*, Vol. 101, No. 7, July 1975, pp. 947-963